JACS
JOURNAL OF THE AMERICAN CHEMICAL SOCIETY
pubs.acs.org/JACS
Article

Synthetic *O*-Acetylated Sialosides and their Acetamido-deoxy Analogues as Probes for Coronaviral Hemagglutinin-esterase Recognition

Zeshi Li,[#] Luca Unione,[#] Lin Liu, Yifei Lang, Robert P. de Vries, Raoul J. de Groot, and Geert-Jan Boons*

Cite This: *J. Am. Chem. Soc.* 2022, 144, 424−435
Read Online

ABSTRACT: *O*-Acetylation is a common modification of sialic acids that can occur at carbons 4-, 7-, 8-, and/or 9. Acetylated sialosides are employed as receptors by several betacoronaviruses and toroviruses, and by influenza C and D viruses. The molecular basis by which these viruses recognize specific *O*-acetylated sialosides is poorly understood, and it is unknown how viruses have evolved to recognize specific *O*-acetylated sialosides expressed by their host. Here, we describe a chemoenzymatic approach that can readily provide sialoglycan analogues in which acetyl esters at C4 and/or C7 are replaced by stabilizing acetamide moieties. The analogues and their natural counterparts were used to examine the ligand requirements of the lectin domain of coronaviral hemagglutinin-esterases (HEs). It revealed that HEs from viruses targeting different host species exhibit different requirements for *O*-acetylation. It also showed that ester-to-amide perturbation results in decreased or loss of binding. STD NMR and molecular modeling of the complexes of the HE of BCoV with the acetamido analogues and natural counterparts revealed that binding is governed by the complementarity between the acetyl moieties of the sialosides and the hydrophobic patches of the lectin. The precise spatial arrangement of these elements is important, and an ester-to-amide perturbation results in substantial loss of binding. Molecular Dynamics simulations with HEs from coronaviruses infecting other species indicate that these viruses have adapted their HE specificity by the incorporation of hydrophobic or hydrophilic elements to modulate acetyl ester recognition.

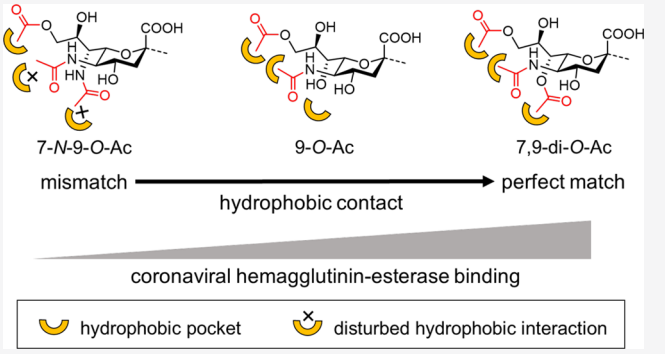

■ INTRODUCTION

Sialic acids are a class of keto-acid sugars having a nine-carbon backbone that exhibit extraordinary structural diversity.[1] They are often found at the termini of glycans of animal tissues with *N*-acetylneuraminic acid (Neu5Ac) and *N*-glycolylneuraminic acid (Neu5Gc) being the most common forms. Neu5Ac is usually attached to galactose (Gal) through an α2,3- or α2,6-linkage, to *N*-acetylgalactosamine (GalNAc) in an α2,6-fashion, or to another Neu5Ac via an α2,8-linkage. Further structural diversity can arise from modifications of the hydroxyls. *O*-Acetylation is the most common form, which can occur at the 4-, 7-, 8-, and/or 9-positions to give rise to up to nine partially *O*-acetylated variants (Figure 1). The expression of these glycotopes is regulated in a tissue- and cell-specific manner via a hitherto unknown mechanism.[2] A growing body of literature has linked *O*-acetylated sialic acids (*O*-Ac-Sias) to a wide range of biological processes such as B- and T-cell immunity,[3,4] cancer drug resistance,[5] and bacterial foraging.[6,7] These biomolecules are also employed as receptors by several betacoronaviruses and toroviruses (subfamily *Orthocoronavirinae* and family *Tobaniviridae*, respectively), and by influenza C and D viruses.[8] Different host species express different repertoires of *O*-acetylated sialosides, which appears to hamper cross species transmission.

Recently, we reported a chemo-enzymatic methodology that can provide sialosides having different patterns of *O*-acetylation.[9] It is based on the chemical synthesis of α2,3-, 2,6-, and 2,8-linked sialosides carrying acetyl esters at C-4, C-7, and C-9, which could readily be diversified by treatment with the hemagglutinin-esterases (HEs) from bovine coronavirus (BCoV) and hepatitis virus strain S (MHV-S) that have 9-*O*- and 4-*O*-acetylesterase activity, respectively, and, in combination with controlled acetyl ester migration from C-7 to C-9, could provide almost any sialate-acetylation pattern. The

Received: September 29, 2021
Published: December 30, 2021

https://doi.org/10.1021/jacs.1c10329
J. Am. Chem. Soc. 2022, 144, 424−435

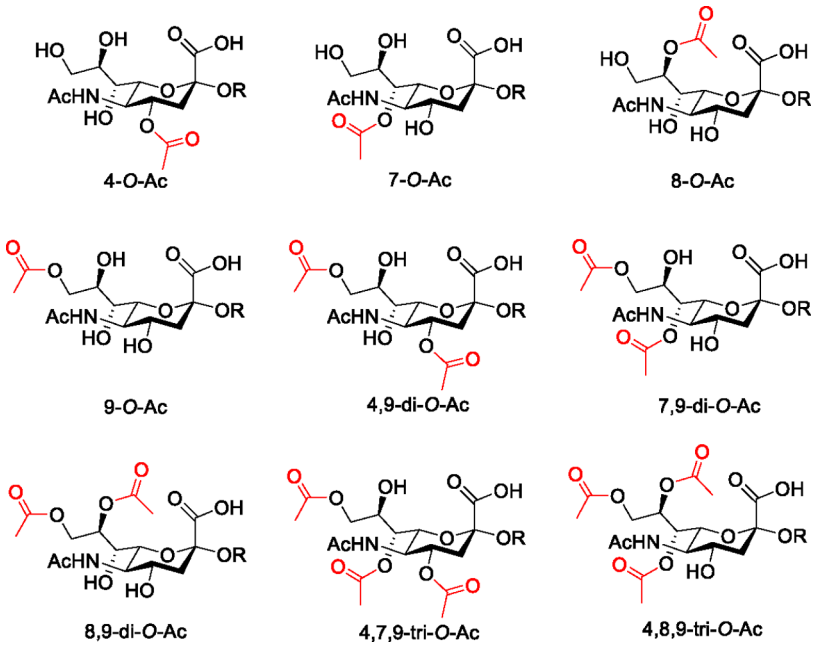

Figure 1. Naturally occurring *O*-acetylated variants of sialic acid.

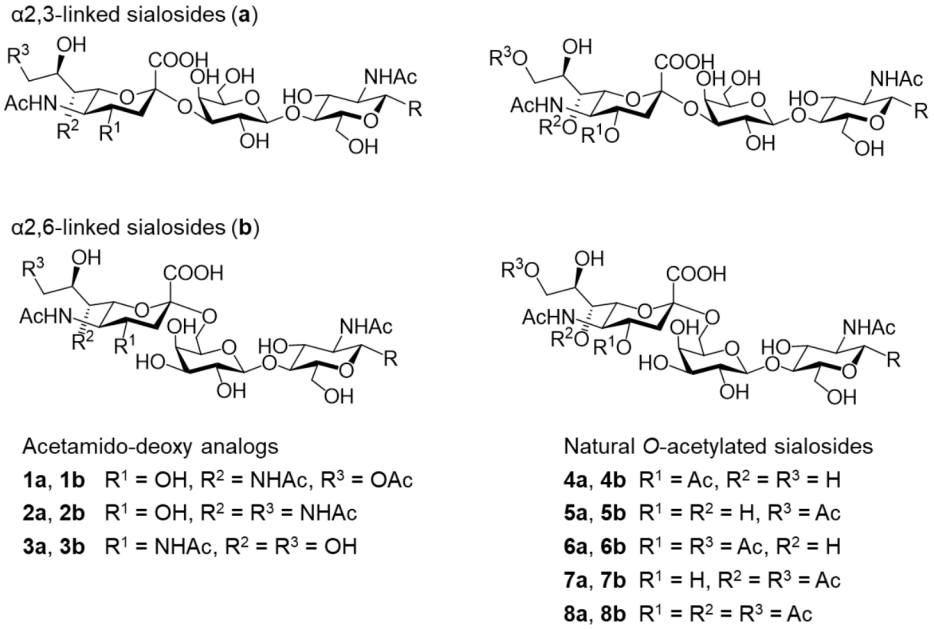

Figure 2. Synthetic *O*-acetylated sialosides and their acetamido-deoxy analogues used in this study. The substituent at the reducing end is not shown for clarity.

resulting collection of *O*-acetylated sialoglycans was printed as a microarray, which was employed to examine the receptor specificities of a group of viruses that engage with *O*-acetylated sialosides of host cells for infection.

For various bioactive molecules, such as acetylcholine[10] and procaine,[11] it has been demonstrated that an acetyl ester can be replaced by an acetamido moiety without loss of recognition and resulting in improved stability. We and others have shown that C9- and C4-acetamido sialosyl analogues are resistant to esterase degradation, overcoming the chemical instability while retaining binding to the virolectins derived from nidoviruses.[12−14] Therefore, we were compelled to develop a chemoenzymatic methodology that can provide easy access to the 7- and 4-deoxy-*N*-acetyl sialosyl analogues **1**−**3** that are linked in an *α*2,3- or *α*2,6-fashion to *N*-acetyl lactosamine (Figure 2). The resulting compounds and corresponding *O*-acetyl-modified sialosides (**4**−**8**) were printed as a glycan microarray, which was probed for recognition by the lectin domain of HEs and spike proteins from bovine, canine, equine, rabbit, and murine coronaviruses and the distantly related bovine torovirus. The array binding studies showed that an 7-*O*-acetyl ester enhances binding for a number of HEs that have an obligatory requirement for 9-*O*-acetylation. Furthermore, it revealed that 7- and 4-*N*-acetamides are not well tolerated by the proteins. Although the acetamide-containing analogues were not well recognized, they proved to be valuable probes for

https://doi.org/10.1021/jacs.1c10329
J. Am. Chem. Soc. 2022, 144, 424−435

Scheme 1. Chemoenzymatic Synthesis of 7-*N*,9-*O*-Acetylated α2,3 (a) and 2,6-Linked (b) Sialosides[a]

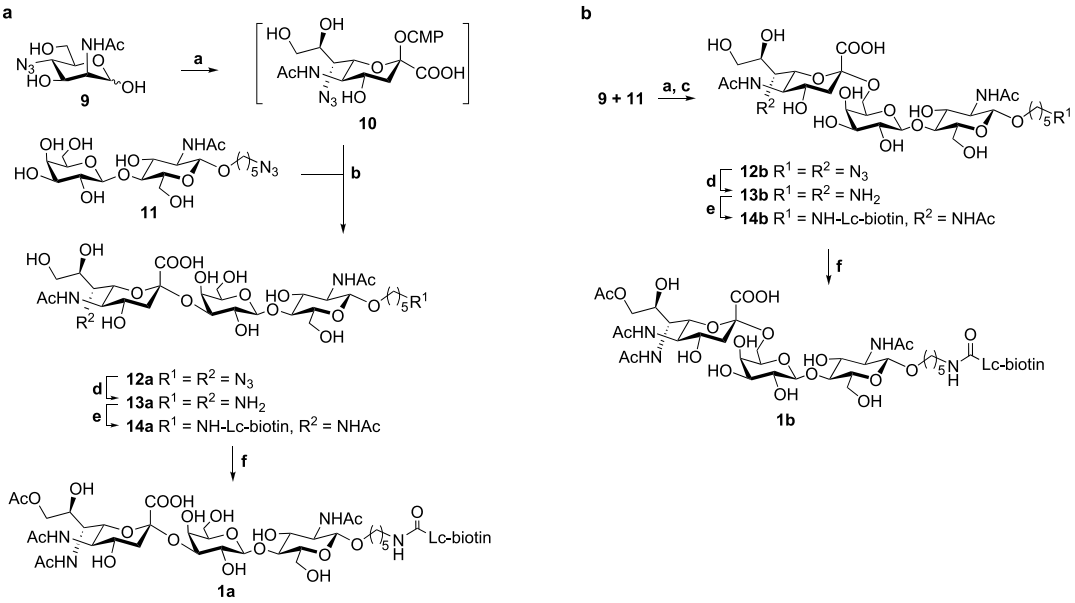

[a]Reaction conditions: a, sodium pyruvate, cytidine 5′-triphosphate (CTP, sodium salt), sialic acid aldolase, CMP-sialic acid synthetase from *N. meningitidis*, 20 mM $MgCl_2$, 0.2 M Tris·HCl buffer, 37°C; b, sialyltransferase PMST1-M144D; isolated yield 77% for **12a**; c, human ST6Gal1; isolated yield, 67% for **12b**; d, H_2, $Pd(OH)_2$, H_2O, 21°C; e, NHS-Lc-biotin (see the Supporting Information for the structure), triethylamine, DMF/H_2O (4:1, v/v), 0 °C, then Ac_2O; isolated yields, 87% for **14a** and 74% for **14b**, over two steps; f, trimethylorthoacetate, toluenesulfonic acid monohydrate, DMSO; isolated yields, 72% for **1a**, 67% for **1b**.

Scheme 2. Chemoenzymatic Synthesis of 7,9-Di-*N*-acetylated α2,3 (a) and 2,6-Linked (b) Sialosides[a]

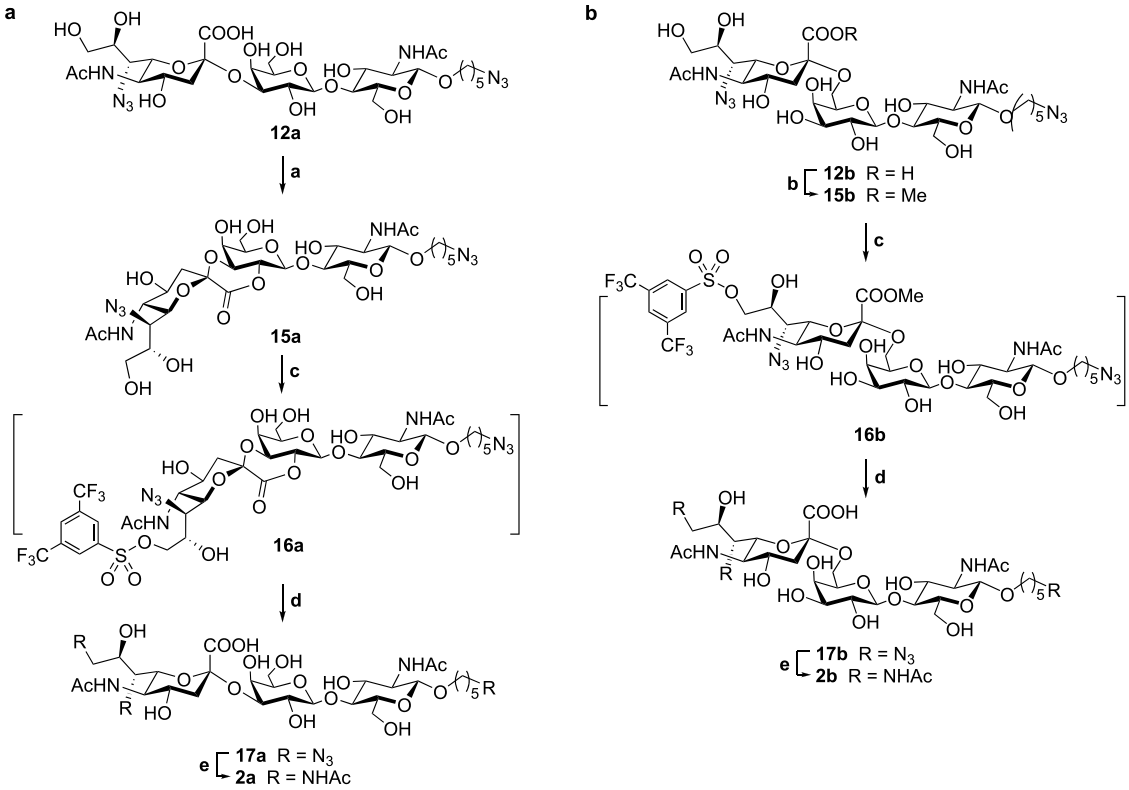

[a]Reaction conditions: a, EDC·HCl, HOBt, DMF, 0−21°C; b, EDC·HCl, HOBt, MeOH, 0−21°C; c, Bu_2SnCl_2, DIPEA, 3,5-bis(trifluoromethyl)-benzenesulfonyl chloride, THF/DMF (8:1, v/v), 0−37°C; d, sodium azide, DMF, 60 °C, then 1 M NaOH, 21 °C; isolated yields, 73% for **17a**, 60% for **17b**, over three steps; e, (i) H_2, $Pd(OH)_2$, H_2O, 21°C; (ii) Ac_2O, triethylamine, DMF/H_2O (4:1, v/v), 0 °C; isolated yields, 84% for **2a**, 88% for **2b**, over two steps.

https://doi.org/10.1021/jacs.1c10329
J. Am. Chem. Soc. 2022, 144, 424−435

Scheme 3. Chemoenzymatic Synthesis of 4-*N*-Acetylated Sialosides α2,3 (a) and 2,6-Linked (b) Sialosides[a]

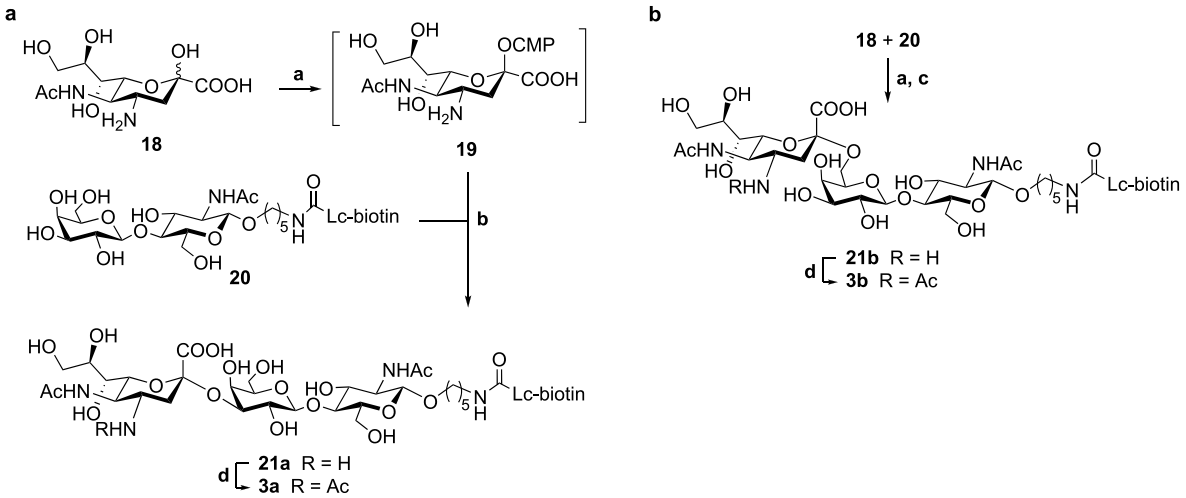

[a]Reaction conditions: a, CTP sodium salt, sialic acid aldolase, CMP-sialic acid synthetase from *N. meningitidis*, 20 mM $MgCl_2$, 0.2 M Tris·HCl buffer, 37 °C; b, PMST1-M144D; c, PMST1-P34H/M144L; d, Ac_2O, triethylamine, DMF/H_2O (4:1, v/v), 0 °C; isolated yields, 71% for **3a**, 52% for **3b**, over two steps.

protein recognition studies. Proton saturation-transfer difference (^{1}H-STD) NMR experiments and molecular modeling of the complex of the HE of BCoV with **1a** and its natural counterpart **7a** revealed that the HE receptor preference is critically governed by the complementarity between acetyl moieties of the sialosides and hydrophobic patches of the lectin with stringent requirements for precise spatial arrangement of these elements. Molecular Dynamics (MD) simulations with HEs from coronaviruses infecting other species indicate that these viruses have adapted their HE specificity for specific forms of *O*-acetylated sialoglycans by the incorporation of hydrophobic or hydrophilic elements to modulate acetyl ester recognition.

■ RESULTS AND DISCUSSION

Synthesis of Sialosides Modified by 7- and 4-Acetamido-deoxy Moieties. We devised a chemoenzymatic strategy for the preparation of **1a**, **1b**, **2a**, and **2b** on the basis of the enzymatic conversion of 4-azido-*N*-acetyl-mannosamine (**9**) into the corresponding CMP-sialic acid derivative, which could be transferred by an appropriate sialyltransferase to the C-3′ or C-6′ position of spacer containing *N*-acetyl lactosamine (**11**) to give **12b** and **12a**. Subsequent regioselective chemical manipulations provided the target compounds (Scheme 1). Thus, condensation of 4-azido ManNAc **1** with pyruvate in the presence of the aldolase from *E. coli* gave 7-azido-sialic acid, which was immediately converted into CMP-Neu5Ac7N_3 (**10**) by reaction with cytidine monophosphate (CMP) catalyzed by CMP-sialic acid synthetase from *Neisseria meningitidis*.[15] The in situ formed donor could readily be employed by the human α2,6-sialyltransferase, ST6Gal1, and sialylation of spacer-containing LacNAc **11** resulted in the efficient formation of **12b**. Human ST3Gal4, which biosynthesizes the α2,3-linked isomer, could not employ CMP-Neu5Ac7N_3 as a donor, and even after a prolonged incubation time, no product formation was detected. These observations indicate that the human sialyltransferases differ in substrate promiscuity and exhibit fine specificities for differentially modified CMP-sialic acid donors. Fortunately, the bacterial sialyltransferase PMST1[16] could readily employ CMP-Neu5Ac7N_3 as a donor, and sialylation of **11** gave 7-azido-containing α2,3-linked sialyl LacNAc **12a**.

The azido moieties of **12a** and **12b** were reduced by hydrogenation using palladium hydroxide to give bis-amine intermediates **13a** and **13b**. The amine on the anomeric linker of the latter compounds was selectively modified with Lc-biotin using the corresponding succinimide ester, which was followed by acetylation of the C7 amine of Neu5Ac using acetic anhydride in the presence of triethylamine, to provide **14a** and **14b** in 87% and 74% overall yields, respectively, without intermediate purification steps.

Compounds **14a** and **14b** were convenient intermediates for the preparation of the target compounds **1a** and **1b**, which have a sialoside modified by a C-7 acetamido moiety and a C-9 acetyl ester. We reason that the C9-hydroxyl of the glycerol chain of Neu5Ac would be the most reactive, and as expected reaction of **14a** and **14b** with trimethylorthoacetate[17] in the presence of toluenesulfonic acid in DMSO resulted in the modification of the C8−C9 diol of the glycerol side chain to give an intermediate orthoester that upon hydrolysis provided **1a** and **1b**, respectively. The compounds were purified by HPLC over a HILIC column to remove residual unreacted C9 nonacetylated starting material. The regioselectivity of the reaction was confirmed by NMR, which demonstrated that the geminal hydrogens at C9 of Neu5Ac had substantially shifted downfield.

The 7-azido sialyl LacNAc **12a** and **12b** were also the starting materials for the 7,9-di-*N*-acetylated analogues **2a** and **2b** using an alternative derivatization procedure (Scheme 2). Thus, treatment of **12a** with EDC·HCl and HOBt in DMF resulted in the formation of lactone **15a**. The methyl ester **15b** was formed by treatment of **12b** with methanol in the presence of EDC·HCl and HOBt.[18] The 9-hydroxyl of Neu5Ac of **15a** and **15b** was modified as a 3,5-bis(trifluoromethyl)-benzenesulfonate by treatment with the corresponding sulfonyl chloride in the presence of Bu_2SnCl_2 and DIPEA to give **16a** and **16b**, respectively.[19] Probably, the reaction proceeds through a dibutyl stannylene acetal, which preferably forms at the C8−C9 diol of the glycerol chain of Neu5Ac, and by limiting the stoichiometry of sulfonyl chloride, **16a** and **16b** are

https://doi.org/10.1021/jacs.1c10329
J. Am. Chem. Soc. 2022, 144, 424−435

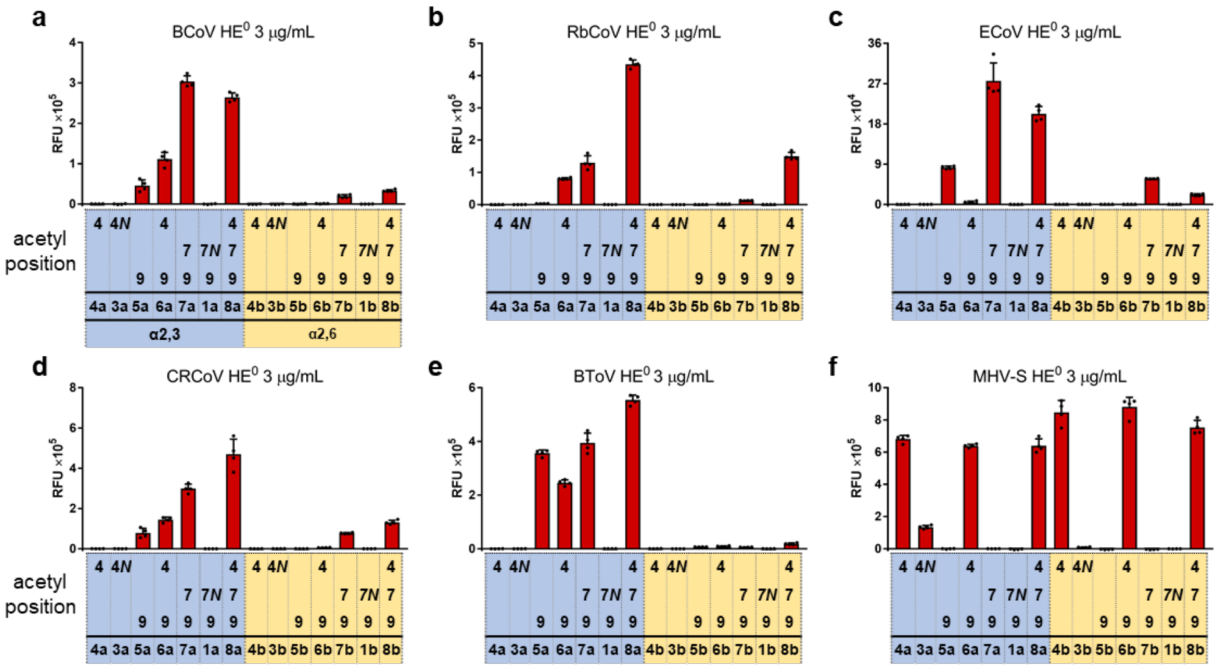

Figure 3. Glycan microarray analysis of BCoV (a), RbCoV (b), ECoV (c), CRCoV (d), BToV (e), and MHV-S (f) HEs binding. HE^0 denotes the esterase-inactive mutant. Sialosides having an α2,3-linkage are shaded in blue, and those with α2,6 are in yellow. *4N* and *7N* in the tables below the bar graphs indicate the corresponding acetamide-deoxy analogues. Relative fluorescence unit (RFU) values are with the background subtracted. The heights of the columns show the background-subtracted average RFUs of four replicate spots. Error bars represent the standard deviation RFUs. Data points for *O*-acetylated sialosides (**4**−**8a** and **b**) were from our previous publication,[9] which were obtained on the same slides with the acetamido-deoxy analogues (**1** and **3a**,**b**). See Figure S1g−n for spike binding. All binding experiments were performed at 4 °C to avoid potential *O*-acetyl migration.

selectively formed. Displacement of the sulfonates **16a** and **16b** by sodium azide followed by hydrolysis of the lactone and methyl esters afforded compounds **17a** and **17b**. The azido moiety of the latter compounds was reduced to an amine by hydrogenation, which was followed by *N*-acetylation using acetic anhydride to give **2a** and **2b** in high overall yield. The successful preparation of the modified sialosides demonstrates that orthoester-mediated *O*-acylation and organotin-catalyzed sulfonylation provide attractive avenues for the regioselective derivatization of a vicinal diol of a highly complex poly hydroxylated compound.

Next, attention was focused on the preparation of compounds **3a** and **3b**, which have an unnatural acetamido moiety at C4 of the sialic acid (Scheme 3). Thus, the 4-amino derivative of Neu5Ac (**18**, see Scheme S1 for the synthesis) was converted into the corresponding derivative of CMP-Neu5Ac **19** by treatment with CTP in the presence of the CMP-sialic acid synthetase. The in situ generated donor could be transferred to biotin-modified LacNAc derivative **20** by the bacterial sialyltransferase PMST1 to provide, after acetylation using acetic anhydride, α2,3-sialosyl analogue **3a**. The corresponding 2,6-sialoside **3b** was prepared by a similar route employing a mutant of PMST1 possessing α2,6-sialylating activity.[20] Interestingly, the two human enzymes could not transfer CMP-Neu5Ac modified by a C4 amine. This observation indicates that such modifications are not tolerated by human sialyltransferases, which may be associated with an absence of 4-*O*-acetylated sialosides in humans.[2] Several studies have shown that derivatization of sialosides at C4 can increase binding of immunoregulatory lectins such as Siglecs[21] and viral glycoproteins including neuraminidases of influenza A viruses.[22] The approaches described here provide convenient synthetic routes to such compounds.

Microarray Analysis of HE Binding. Having successfully prepared a range of sialoglycan analogues, attention was focused on the construction of a microarray to probe interactions with hemagglutinin-esterases (HE) of *Embecoviruses* from different host species. *Embecoviruses*, which is a subgenus of the *Coronaviridea*, have a broad host range and can infect human, bovine, canine, equine, murine, and rabbits. In addition to their spike (S) protein, *Embecoviruses* encode a hemagglutinin-esterase (HE)[23] that recognizes *O*-acetylated sialic acid via a lectin domain, and hydrolyze sialate-*O*-acetyl esters via an esterase domain. Fine-tuned binding preferences of HEs for different forms of *O*-acetylated sialic acids have been observed for *Embecoviruses* targeting distinct host species,[9] which likely is a result of adaptation to the *O*-acetyl sialoglycome of the host.

Compounds **1**−**3a**,**b** and a panel of previously prepared *O*-acetylated sialosides **4**−**8a**,**b** (Figure 2) were employed to create a microarray to examine the effect of *O*-to-*N* substitution on protein recognition. The sialosides were printed on streptavidin-coated glass slides, and the resulting microarray was exposed to Fc-fusion proteins of inactive esterase (HEs) domains from bovine, equine, canine, and rabbit betacoronaviruses (BCoV, ECoV, CRCoV, and RbCoV, respectively), bovine toroviruses (BToV),[9,24−26] and murine hepatitis virus strain S (MHV-S).[12] Detection of binding was accomplished using an anti-Fc antibody tagged with Alexa-Fluor-647.

BCoV, RbCoV, ECoV, CRCoV, and BToV HEs recognized 2,3-linked sialoside **7a**, which has acetyl esters at C7 and C9. Replacement of the acetyl ester at C7 by an acetamide to give

https://doi.org/10.1021/jacs.1c10329
J. Am. Chem. Soc. 2022, 144, 424−435

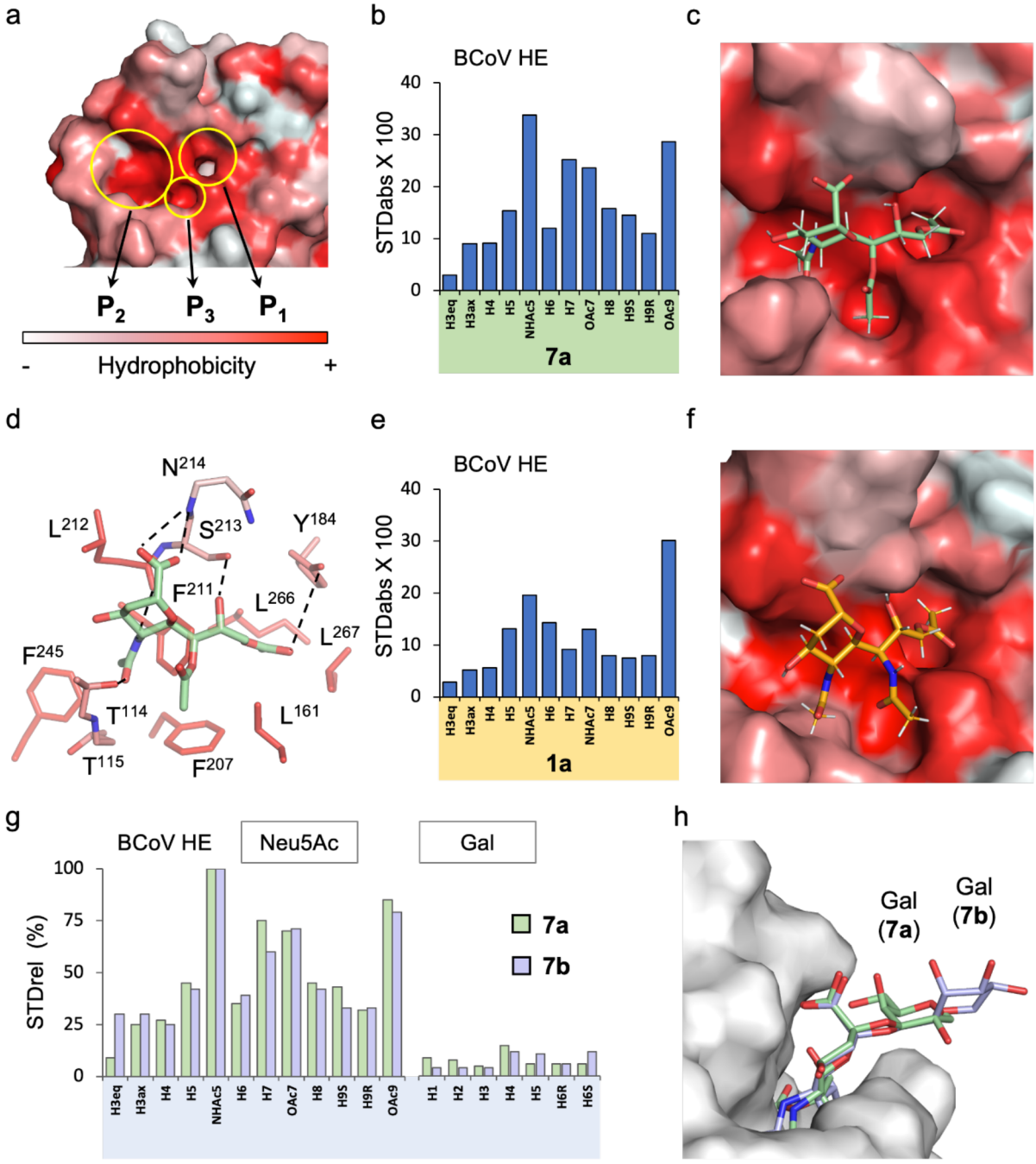

Figure 4. Structural basis of the BCoV HE:receptor interaction. (a) Surface representation of the BCoV HE apo form (pdb code 3CL4).[24] The protein surface is colored according to the amino acids' hydrophobicity. The three hydrophobic pockets are indicated with yellow circles. (b) ^{1}H-STD NMR profile of compound **7a** in complex with BCoV HE. The heights of the columns represent the absolute STD (STDabs) values. (c) Surface and stick representation of the BCoV HE lectin site in complex with compound **7a** as modeled by MD simulations. The Gal and GlcNAc residues are not shown for clarity. (d) Atomic details of the BCoV HE:**7a** interactions as determined by ^{1}H-STD NMR and MD simulations. (e) ^{1}H-STD NMR profile of the acetamido-deoxy analogue compound **1a** in complex with BCoV HE. (f) Surface and stick representation of the BCoV HE lectin site in complex with compund **1a** as determined by ^{1}H-STD NMR. Note the different binding pose with respect to the natural compound **7a**. The main differences reside in the packing of the Neu5Ac-7-*O*-Ac and 5-NHAc groups. (g) Comparison of the relative (%) ^{1}H-STD NMR profiles obtained for compounds **7a** and **7b**. The largest value given rise to by 5-NHAc of **7a** is set as 100%. (h) Superimposition of the MD-derived structures for BCoV HE in complex with **7a** (green) and **7b** (blue). Note the proximity of the galactose ring to the protein for **7a** with respect to **7b**. The GlcNAc residues are hidden for clarity.

compound **1a** abolished binding (Figure 3a−e). Similar observations were made for 2,6-linked sialosides (**7b** vs **1b**). MHV-S HE has an obligatory requirement for 4-*O*-aceylation.[12] The ester-to-amide substitution at C4 (compounds **3a** and **3b**) was tolerated by MHV-S HE but resulted in substantially weaker binding as compared to the parent compounds **4a** and **4b** (Figure 3f). These results indicate that, unlike *N*-acetylation at C9,[13] acetamides at C-7 and C-4 are not appropriate isosteres of acetyl esters for HE recognition.

https://doi.org/10.1021/jacs.1c10329
J. Am. Chem. Soc. 2022, 144, 424−435

The microarray data showed that the different HEs have different requirements for 7-*O*-acetylation. In the case of BCoV, RbCoV, ECoV, and CRCoV HEs, 7-*O*-acetylation (as in **7a** and **b**) increased binding, while BToV HE was unaffected by this modification. It also revealed the multifaceted roles of 4-*O*-acetylation in the regulation of HE recognition for the closely related *Embecoviruses* BCoV, CRCoV, RbCoV, and ECoV. The HEs of the first two viruses tolerated this modification and exhibited a similar pattern of receptor recognition. On the other hand, the presence of a 4-*O*-acetyl ester substantially increased binding for RbCoV HE, and α2,3-linked 4,7,9-tri-*O*-acetylated Neu5Ac derivative **8a** was the strongest binder (Figure 3b). In contrast, the same modification decreased binding of ECoV HE (Figure 3c, **6a** vs **5a**). However, in this case, the unfavorable effect of 4-*O*-acetylation could be alleviated by the presence of a 7-*O*-acetyl ester (**8a** vs **6a**). The glycan array was also probed for spike proteins from BCoV, RbCoV, ECoV, and CRCoV (Figure S1). While the spike of BCoV bound to 9-mono and 7,9-di-*O*-acetylated sialosides equally well, it exhibited only weak binding when C7 is modified by an acetamide moiety. For the spike proteins from RbCoV, ECoV, and CRCoV, the presence of an acetyl ester decreases the binding, while compounds having a 7-acetamide substitution did not produce any responsiveness. Probing the microarray at a lower protein concentration (1 μg/mL, Figure S1a−f) showed in each case a dose response effect, indicating that saturation of binding had not been reached.

Structural Basis of BCoV HE−Receptor Interactions. The HEs of bovine, canine, equine, and rabbit coronaviruses require an acetyl ester at C9 for binding but exhibit different requirements for additional acetyl esters. The understanding of *O*-Ac-Sia engagement by viral receptor binding proteins at a structural level is largely limited to 9-monoacetylated sialic acid. An X-ray crystal structure of BCoV HE in complex with sialic acid carrying acetyl ester at C-4 and C-9 (pdb code 3CL5) has provided some insight into the recognition of this class of glycan.[24] A deep pocket (P_1) defined by Tyr^{184}, Leu^{266}, and Leu^{267} accommodated the 9-*O*-acetyl ester and the glycerol side chain. The 5-*N*-acetyl moiety is placed in a wide cavity (P_2) defined by Phe^{245}, Leu^{212}, and Phe^{211}, which is sufficiently large to host an additional *O*-acetyl ester at C4. The complex is stabilized by hydrogen bonds between the C5-amide and Leu^{212}, the C1-carboxylate and Asn^{214}, and the C8 oxygen and Ser^{213}.

The structural data do not provide a rationale for the substantial higher affinity for sialosides having an acetyl ester at C7. Furthermore, there are no reported structures of the HEs from canine, equine, and rabbit coronaviruses, and it is not understood at a structural level how these closely related proteins have adapted to different forms of *O*-acetylated sialosides. Here, we employed NMR experiments, homology modeling, and molecular dynamics (MD) simulations to understand, at a molecular level, the receptor specificities of HEs for various coronaviruses.

Examination of the receptor binding site of the lectin domain of apo BCoV HE (pdb code 3CL4) indicates the presence of an additional hydrophobic pocket (P_3), defined by Phe^{207}, Thr^{114}, and Leu^{161}, which may accommodate a C-7 acetyl ester (Figure 4a) and may be responsible for the higher affinity of BCoV HE for 7,9-di-*O*-acetylated sialosides. To validate this hypothesis, saturation transference difference (^{1}H-STD NMR) and MD simulations were performed for the complex of BCoV HE with 7,9-di-*O*-acetylated sialosides **7a** and **7b**. Furthermore, the ester-to-amide perturbation strategy[27,28] was employed to demonstrate a stringent requirement of proper positioning of hydrophobic elements for HE:sialic acid complex formation.

The interaction of BCoV HE with the α2,3-linked 7,9-di-*O*-acetylated sialoside (**7a**), the α2,6-linked 7,9-di-*O*-acetylated sialoside (**7b**), and the 7-*N*,9-*O*-acetylated analogue (**1a**) was studied by ^{1}H-STD NMR spectroscopy to provide atomic details of the interaction between the acetylated sialosides and the HE. The ^{1}H-STD NMR experiments were performed using a BCoV HE hydrolase-inactive form[9] at 30 μM concentration in 50 mM PBS, in D_2O (pD 7.2) using a lectin/ligand ratio of 1:50. The temperature was set to 298 K. STD experiments were performed on a 600 MHz Bruker spectrometer, using standard Bruker pulse sequences without water suppression or a protein spin-lock filter. Protein saturation was achieved with a Gaussian-shaped pulse of 40 ms during a saturation time of 2 s. The on-resonance frequency was set at the aliphatic region (0.76 ppm), and the off-resonance frequency was set at 100 ppm (for further details, see Figure S1a and the General Procedure section in the Supporting Information).

For compound **7a** (Figures 4b and S2b), the strongest STD signals arose from the methyl groups of the 5-*N*-, 9-*O*-, and 7-*O*-acetyl moieties and from the H7 of sialic acid, indicating that ligand binding is mainly governed by the acetyl moieties of the sialoside. Moderate STD signals were observed for the H5, H6, H8, and $H9_S$ of the sialoside, which indicate that these atoms face the protein surface. Weak STD signals were detected for H3eq, H3ax, H4, and $H9_R$, indicating that these atoms are solvent exposed. Even weaker STD signals were detected for the underlying galactoside (Gal), while those of the *N*-acetyl glucosamine (GlcNAc) residue were not present, indicating that the underlying glycan makes only marginal contacts with the protein.

^{1}H-STD NMR experiments with α2,6-linked compound **7b** gave results similar to those for the α2,3-linked analogue **7a** (Figures 4g and S2d). The intensity of the STD signals of the sialic acid residue was essentially the same as that for **7a**, while those of the galactose residue were also weak. Nonetheless, differences were observed, and for compound **7b** the strongest signals of Gal arose from $H6_S$, H5, and H4, whereas for compound **7a** the strongest signals corresponded to H4, H1, and H2. These results indicate differences in the positioning of the Gal residues between the two binding complexes, where in the case of **7b** the C1−C4 side of the galactosyl ring points to the protein surface, yet for **7a** it is the C4−C6 side.

Next, the molecular mechanisms of poor binding of the ester-to-amide substitution at C7 were investigated. The ^{1}H-STD NMR spectrum of 7-*N*-acetyl analogue **1a** with BCoV HE showed much weaker STD intensities for the methyl groups of the C7 and C5 substituents as compared to **7a** (Figures 4e and S2c). The sialic acid backbone hydrogens (H3−H9) were less affected, whereas the STD signal for the C9 acetyl ester was unchanged. These observations indicate that, despite that C9 acetyl ester being properly anchored in the P1 pocket, the acetamide at C7 hinders optimal interactions with the P2 and P3 pockets, which likely results in much weaker binding.

In Silico Studies of BCoV, RbCoV, and ECoV Receptor Preferences. The differences in receptor preference of BCoV, RbCoV, and ECoV HEs are remarkable given the high sequence similarity of their lectin domains (96%). BCoV HE binds 7,9-di- (**7a**) and 4,7,9-tri-*O*-acetylated (**8a**) Neu5Ac

https://doi.org/10.1021/jacs.1c10329
J. Am. Chem. Soc. 2022, 144, 424−435

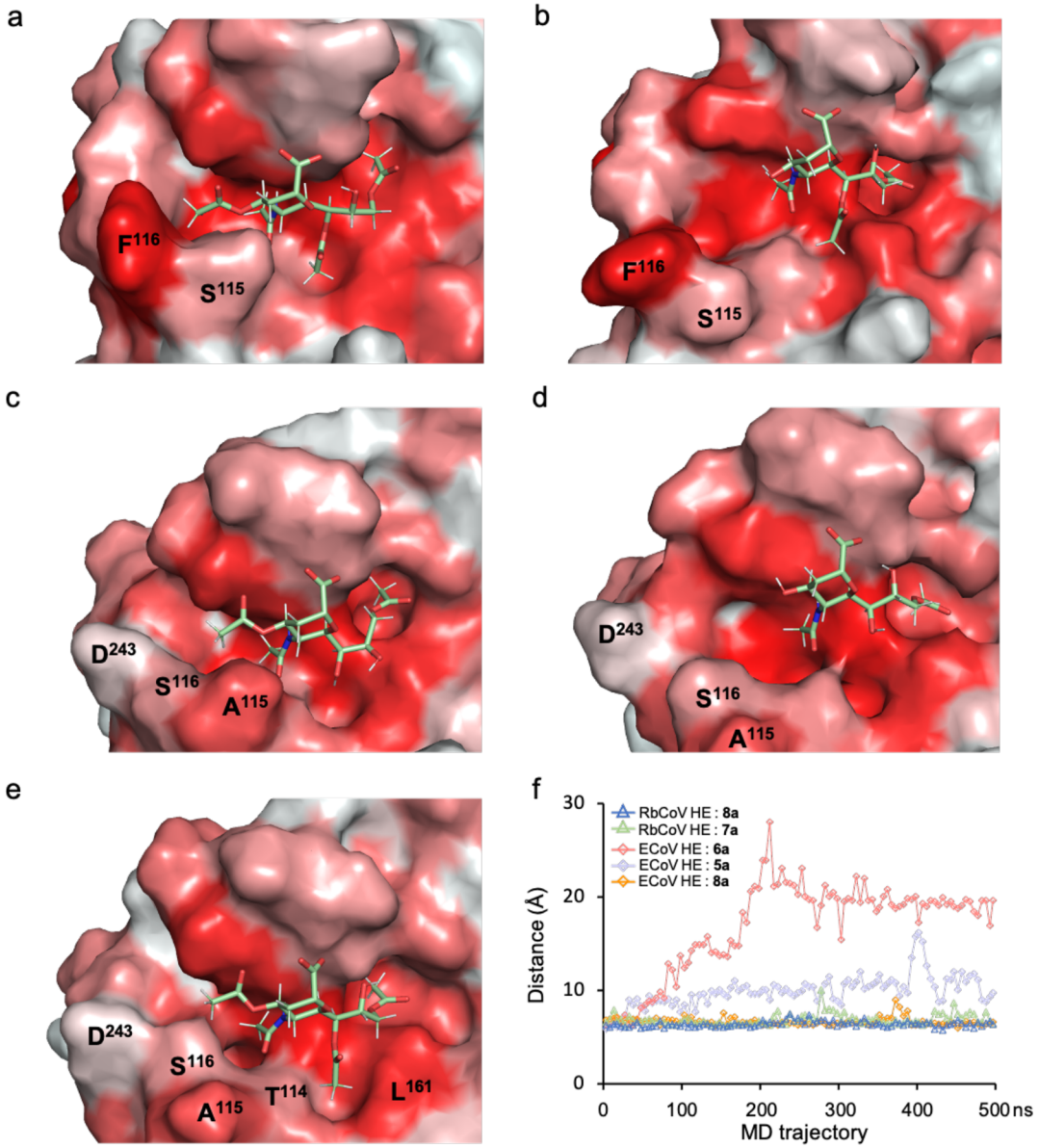

Figure 5. Structural models of RbCoV and the ECoV HE:receptors interaction. (a) Structure of the RbCoV HE lectin domain in complex with compound **8a**. Note the proximity of the F116 side chain to the Neu5Ac-4-*O*-Ac-methyl group favorable for CH−π interactions. (b) Structure of the RbCoV HE lectin domain in complex with compound **7a**. (c) Structure of the ECoV HE lectin domain in complex with compound **6a**. (d) Structure of the ECoV HE in complex with compound **5a**. (e) Structure of the ECoV HE lectin domain in complex with **8a**. All of the structures correspond to a selected frame from the MD simulations. Gal and GlcNAc residues are hidden for clarity. (f) Stability of the complexes along the MD simulations. The curves represent the distance between the centers of mass of the Neu5Ac residue and Phe^{211} along the MD trajectory. Phe^{211} is the key residue composing the lectin binding site and was arbitrarily chosen among the others. The MD simulations of ECoV HE with **6a** and **5a** show a weak binding. In contrast, the short and constant distance of ECoV HE with **8a** indicates a stable binding pose. Similarly, in RbCoV HE, the graphic shows a more stable pose for the tri-*O*-acetylated compound **8a** than that in the case of the di-*O*-acetylated compound **7a**.

derivatives equally well, whereas RbCoV HE showed a strong preference for the 4,7,9-tri-*O*-acetylated form. In contrast to the RbCoV and BCoV, C4 acetylation reduced binding to ECoV HE virolectin (Figure 3). We performed 500 ns Molecular Dynamics simulations of complexes of the HEs with relevant sialosides in a 10 Å octahedral box of explicit TIP3P waters and compared the resulting structures to uncover the moleculer basis of receptor preferences.

BCoV HE. Molecular Dynamics (MD) simulations were performed to obtain a structural model of BCoV HE complexed with **7a** and **7b**. The crystallographic structure of BCoV HE in complex with 4,9-*O*-Ac-Sia is available (pdb code 3CL5). Therefore, the 7,9-di-*O*-acetylated sialosides were superimposed onto the corresponding monosaccharide in the crystal structure, and the resulting binding poses were minimized and subjected to MD simulation in explicit water using the AMBER molecular simulation program.[29] The GLYCAM force field was employed for the glycan,[30] and the 14SB force field[31] was used for the protein using periodic boundary conditions in explicit water.[32] The resulting structures (Figure 4c) are in excellent agreement with the STD NMR-derived epitope mapping and recapitulated observations made by X-ray crystallography. The 9-*O*-acetyl methyl group and the glycerol chain docked into the P_1 pocket

https://doi.org/10.1021/jacs.1c10329
J. Am. Chem. Soc. 2022, 144, 424−435

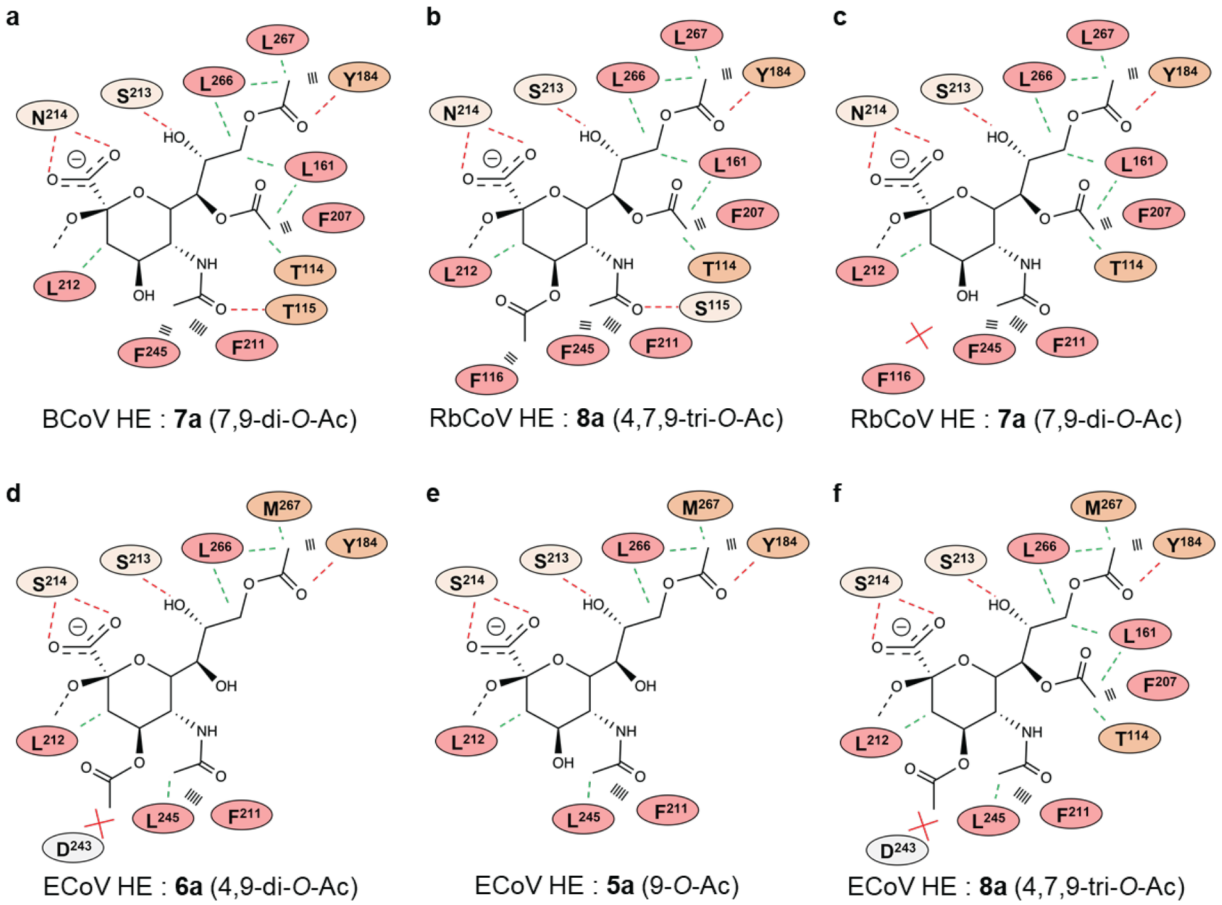

Figure 6. Schematic representation of the interactions between different acetylated sialosides and the lectin domain of the HEs from BCoV (a), RbCoV (b and c), and ECoV (d–f). Red dashed lines indicate the hydrogen-bonding interactions, green dashed lines represent the hydrophobic contacts, black parallel lines indicate the CH–π interactions, and red crosses show the unfavorable interactions.

defined by Tyr[184], Leu[266], and Leu[267] (see Figures S3–S5 for analyses of the key hydrophobic interaction). The 5-*N*-acetyl fits into the wide P_2 cavity defined by Phe[245], Leu[212], and Phe[211] (Figure S6). Furthermore, the sialic acid makes polar interactions through a hydrogen-bonding network with residues Thr[115], Tyr[184], Leu[212], Ser[213], and Asn[214] (Figure 4d, Table S1, and Figure S9). As anticipated, the MD simulations showed a third hydrophobic cavity (P_3), defined by Phe[207], Thr[114], and Leu[161], which can accommodate the additional acetyl ester at C7 (Figures S7 and S8, summarized in Figure 6a). Remarkably, the latter residues are in two loop regions that contribute to the architecture of the glycan binding pocket and define the receptor specificity. Our structural model reveals a precise alignment of the hydrophobic patch in BCoV HE with the acetyl moieties of the sialoglycans. Comparison of the MD trajectory of BCoV HE in complex with **7a** or **7b** (Figure S10) revealed that in the case of α2,3-isomer the Gal moiety contributes to protein binding through transient intermolecular hydrogen-bond interactions that mainly involve either Asn[214] or Lys[163]. In the case of the α2,6-isomer, the Gal ring is mainly solvent exposed due to a longer and more flexible glycosidic linkage (Figure 4h). Thus, the different modes of protein–carbohydrate contacts, possibly arising from the distinct topologies of the glycans, may account for differences in the avidity of HEs for α2,3- and 2,6-linked sialosides.[33]

A similar computational approach was used to obtain a model for the complex of the 7-*N*,9-*O*-acetylated analogue **1a** with BCoV HE. The MD trajectory could not be ascribed to a unique binding mode. Therefore, the NMR results were used to extract from the MD simulation a three-dimensional model that fits the experimental data. The resulting structure of the BCoV HE:**1a** complex (Figure 4f) showed that the polar amide function at the C7 provokes an unfavorable contact with the hydrophobic patch (P_3) of the protein precluding proper interactions with the side chains of Leu[161] and Thr[114]. To minimize these unfavorable interactions, the glycerol chain tilted and the Neu5Ac ring moved away from the protein binding pocket, while keeping the C9 methyl group in the P1 pocket. In this binding pose, the acetamide moiety at C5 pushes away Thr[115], resulting in an open cavity at the sialic acid binding site. This mode of binding is consistent with the observed ^{1}H-STD NMR signal, which showed a substantial decrease in STD signal intensities especially for the H7 and CH_3 groups of the acetyl esters at C7 and C5, while that of C9 was unperturbed. Interestingly, the increase in the STD signal of H6 agrees with the proposed binding pose that places this atom closer to the protein surface.

The data demonstrate that an acetamide at C-7 of Neu5Ac is not a proper isostere of the corresponding acetyl ester. It has a slightly increased size and is more hydrophilic and conformationally rigid.[28] Such perturbations greatly reduced the binding of the 7-*N*-acetylated analogue **1a**, highlighting that HE:*O*-Ac-Sia interactions are governed by the precise positioning of sialate-acetyl groups in the hydrophobic pockets of the protein.

https://doi.org/10.1021/jacs.1c10329
J. Am. Chem. Soc. 2022, 144, 424–435

RbCoV HE. An X-ray crystal structure of RbCoV has not been reported, and therefore a homology model was generated using the crystal structure of BCoV HE as a template.[34−36] The resulting apo protein was subjected to a minimization protocol employing the AMBER suite of programs. Next, the *O*-acetylated sialosides **7a** and **8a** were placed into the ligand binding pocket by molecular alignment with the BCoV HE crystal structure, and the generated complexes were subjected to MD simulations as described above.

For both ligands, the MD simulations showed stable binding poses in which the acetyl esters at positions 9, 5, and 7 established hydrophobic interactions with the P_1, P_2, and P_3 pockets, respectively. However, key differences were observed. For the triacetylated **8a**, the hydroxyl of the side chain of Ser^{115} engaged with the acetamide at C5 via a hydrogen bond with the carbonyl oxygen (Table S2 and Figure S11), while the aromatic ring of Phe^{116} established a CH−π interaction with the acetyl ester at C4 (Figures 5a and S12). On the other hand, the complex with **7a** (see Table S3 and Figure S13 for hydrogen-bonding interactions) placed the polar hydroxyl group at C4 toward the hydrophobic Phe^{116}, and this unfavorable contact pushed the Phe^{116} and the contiguous Ser^{115} residue apart, leaving a wide open cavity and thus precluding hydrogen-bond interaction between the Ser^{115} and the acetamide at the C5 of the sialoside (Figure 5b). These results demonstrate that complementarity of the three acetyl moieties at C4, C7, and C9 and the hydrophobic pockets of RbCoV HE are critical for ligand specificity (summarized in Figure 6b and c).

ECoV HE. Finally, we explored the structural elements important for ECoV HE binding. Mono-, di-, and tri-*O*-acetylated sialosides **5a**, **6a**, and **8a** were docked into the binding site of ECoV HE obtained by homology modeling (Figure 5c−e, respectively). MD simulations revealed important differences in the ECoV HE binding site when compared to that of BCoV and RbCoV HEs due to key mutated residues in the loop in close proximity to C4 of Neu5Ac. Among these, Thr^{243}Asp introduces a negative charge, which disrupts protein−ligand contacts with **6a** due to a close proximity to the hydrophobic acetyl ester at C4 of Neu5Ac. Moreover, in ECoV HE, the Ala^{115}, which substitutes either Thr or Ser in BCoV and RbCoV, respectively, cannot engage with the acetamide at C5 through hydrogen bonding, reducing the number of intermolecular interactions. In agreement with the array data, MD simulations of the ECoV HE with either **6a** and **5a** resulted in loose poses (Figure 5f; see Tables S4 and S5 and Figures S14 and S15 for the hydrogen-bonding interactions). The MD trajectory of compound **8a** showed tighter binding mainly due to hydrophobic interactions of the acetyl ester at C7 with the side chains of Leu^{161} and Thr^{114} (Figure 5f; see Table S6 and Figure S16 for the hydrogen-bonding interactions and Figures S17−S19 for analyses of the key hydrophobic interactions). Thus, for ECoV HE, the binding depends even more on interactions between the *O*-acetyl moieties and the surrounding hydrophobic side chains. Consequently, the binding enhancing effect of 7-*O*-acetylation became more profound, as was demonstrated in the microarray and the MD simulation of ECoV HE in complex with 4,7,9-tri-*O*-acetylated sialoside (Figure 5e), in which the disadvantageous effect of C4-acetylation was overruled by the presence of a 7-*O*-acetyl and its interaction with Leu^{161} and Thr^{114} (summarized in Figure 6d−f).

Figure 6 summarizes the hydrogen bonding, hydrophobic contacts, CH−π interactions, and unfavorable interactions of BCoV, RbCoV, and ECoV with various *O*-acetylated sialosides and provides a rationale for their binding preferences.

■ CONCLUSION

Coronaviruses (CoVs) pose great zoonotic threats, and in particular viruses of the subgenus *Embecovirus* have a remarkable ability to cross species barriers.[37] These viruses attach to *O*-acetylated sialoglycans via a spike protein for cell entry and membrane fusion. They also express a hemagglutinin-esterase (HE), which acts as a receptor-destroying enzyme. HE harbors a lectin domain that contributes to virion attachment and enhances the sialate-*O*-acetylesterase activity of clustered sialosides. The receptor specificity of the lectin domain of HE is critically associated with host specificity;[9,26] however, the molecular basis for such preferences is poorly understood. Here, we present an integrated approach to investigate the molecular mechanisms by which HEs recognize specific *O*-acetylated sialosides. It employs a range of *O*-acetylated sialoglycans and analogues in which acetyl esters at C7 and C4 are replaced by acetamides. The latter compounds were prepared by a chemoenzymatic strategy, in which the acetamides were installed by highly regioselective and late-stage chemical modifications. Glycan microarray binding studies demonstrated the modified sialoglycans exhibit much lower affinities as compared to their natural counterparts. The ester-to-amide replacement strategy made it possible to examine the fidelity of recognition of *O*-acetylated sialosides. In particular, ^{1}H-STD NMR and MD simulations demonstrated that the fine specificities of different *O*-acetylation forms of closely related proteins arise from hydrophobic patches that can accommodate sialate-*O*-acetyl moieties. Optimal binding is only achieved when all sialate-*O*-acetyl moieties align with the hydrophobic patches of the proteins. A small perturbation in such an alignment, as introduced by an ester-to-amide replacement, greatly reduces binding. HEs from CoVs infecting different host species exhibit different preferences for sialate-*O*-acetyl patterns. Our findings provide insights into how receptor binding selectivities lead to viral adaptation to the host's sialoglycome.[37] It paves the way to specificity-based engineering of these viral glycoproteins for in situ detection of a select population of *O*-Ac-Sias.[2,38] It also offers opportunities to design inhibitors for HEs, which may pose antiviral properties. The *O*-to-*N* substitution may offer valuable tools to examine molecular recognition by other proteins such as ficolins[39] and anti-*O*-Ac-Sia antibodies.[40] It is known that immunoregulatory lectins, such as Siglecs,[21] and viral glycoproteins including neuraminidases of influenza A viruses[41] tolerate modifications at the C4 of sialosides, which provides opportunities to develop high affinity ligands. The synthetic approaches described here provide avenues for the development of such compounds.

■ ASSOCIATED CONTENT

Supporting Information

The Supporting Information is available free of charge at https://pubs.acs.org/doi/10.1021/jacs.1c10329.

Data supporting the findings of this study (PDF)

https://doi.org/10.1021/jacs.1c10329
J. Am. Chem. Soc. 2022, 144, 424−435

AUTHOR INFORMATION

Corresponding Author

Geert-Jan Boons − *Department of Chemical Biology and Drug Discovery, Utrecht Institute for Pharmaceutical Sciences, Utrecht University, Utrecht 3584 CG, The Netherlands; Complex Carbohydrate Research Center, University of Georgia, Athens, Georgia 30602, United States; Bijvoet Center for Biomolecular Research, Utrecht University, Utrecht 3584, The Netherlands; Chemistry Department, University of Georgia, Athens, Georgia 30602, United States;* orcid.org/0000-0003-3111-5954; Email: gjboons@ccrc.uga.edu, g.j.p.h.boons@uu.nl

Authors

Zeshi Li − *Department of Chemical Biology and Drug Discovery, Utrecht Institute for Pharmaceutical Sciences, Utrecht University, Utrecht 3584 CG, The Netherlands*

Luca Unione − *Department of Chemical Biology and Drug Discovery, Utrecht Institute for Pharmaceutical Sciences, Utrecht University, Utrecht 3584 CG, The Netherlands*

Lin Liu − *Complex Carbohydrate Research Center, University of Georgia, Athens, Georgia 30602, United States;* orcid.org/0000-0002-0310-5946

Yifei Lang − *Virology Division, Department of Biomolecular Health Sciences, Faculty of Veterinary Medicine, Utrecht University, Utrecht 3584 CL, The Netherlands*

Robert P. de Vries − *Department of Chemical Biology and Drug Discovery, Utrecht Institute for Pharmaceutical Sciences, Utrecht University, Utrecht 3584 CG, The Netherlands*

Raoul J. de Groot − *Virology Division, Department of Biomolecular Health Sciences, Faculty of Veterinary Medicine, Utrecht University, Utrecht 3584 CL, The Netherlands*

Complete contact information is available at: https://pubs.acs.org/10.1021/jacs.1c10329

Author Contributions

[#]Z.L. and L.U. contributed equally.

Notes

The authors declare no competing financial interest.

ACKNOWLEDGMENTS

This work was supported by TOP-PUNT Grant 718.015.003 of The Netherlands Organization for Scientific Research (G.-J.B.); the Human Frontier Science Program Organization (HFSP) grant LT000747/2018-C (L.U.); ECHO Grant 711.011.006 of the Council for Chemical Sciences of The Netherlands Organization for Scientific Research (R.J.d.G.); and the China Scholarship Council 2014-03250042 (Y.L.).

REFERENCES

(1) Schauer, R.; Kamerling, J. P. Exploration of the sialic acid world. *Adv. Carbohydr. Chem. Biochem.* **2018**, *75*, 1−213.

(2) Langereis, M. A.; Bakkers, M. J.; Deng, L.; Padler-Karavani, V.; Vervoort, S. J.; Hulswit, R. J.; van Vliet, A. L.; Gerwig, G. J.; de Poot, S. A.; Boot, W.; van Ederen, A. M.; Heesters, B. A.; van der Loos, C. M.; van Kuppeveld, F. J.; Yu, H.; Huizinga, E. G.; Chen, X.; Varki, A.; Kamerling, J. P.; de Groot, R. J. Complexity and diversity of the mammalian sialome revealed by nidovirus virolectins. *Cell Rep.* **2015**, *11* (12), 1966−1978.

(3) Cariappa, A.; Takematsu, H.; Liu, H.; Diaz, S.; Haider, K.; Boboila, C.; Kalloo, G.; Connole, M.; Shi, H. N.; Varki, N.; Varki, A.; Pillai, S. B cell antigen receptor signal strength and peripheral B cell development are regulated by a 9-O-acetyl sialic acid esterase. *J. Exp. Med.* **2009**, *206* (1), 125−138.

(4) Wipfler, D.; Srinivasan, G. V.; Sadick, H.; Kniep, B.; Arming, S.; Willhauck-Fleckenstein, M.; Vlasak, R.; Schauer, R.; Schwartz-Albiez, R. Differentially regulated expression of 9-*O*-acetyl GD3 (CD60b) and 7-*O*-acetyl-GD3 (CD60c) during differentiation and maturation of human T and B lymphocytes. *Glycobiology* **2011**, *21* (9), 1161−1172.

(5) Parameswaran, R.; Lim, M.; Arutyunyan, A.; Abdel-Azim, H.; Hurtz, C.; Lau, K.; Muschen, M.; Yu, R. K.; von Itzstein, M.; Heisterkamp, N.; Groffen, J. *O*-acetylated *N*-acetylneuraminic acid as a novel target for therapy in human pre-B acute lymphoblastic leukemia. *J. Exp. Med.* **2013**, *210* (4), 805−819.

(6) Robinson, L. S.; Lewis, W. G.; Lewis, A. L. The sialate *O*-acetylesterase EstA from gut Bacteroidetes species enables sialidase-mediated cross-species foraging of 9-*O*-acetylated sialoglycans. *J. Biol. Chem.* **2017**, *292* (28), 11861−11872.

(7) Nguyen, T.; Lee, S.; Yang, Y. A.; Ahn, C.; Sim, J. H.; Kei, T. G.; Barnard, K. N.; Yu, H.; Millano, S. K.; Chen, X.; Parrish, C. R.; Song, J. The role of 9-*O*-acetylated glycan receptor moieties in the typhoid toxin binding and intoxication. *PLoS Pathog.* **2020**, *16* (2), No. e1008336.

(8) Wasik, B. R.; Barnard, K. N.; Parrish, C. R. Effects of sialic acid modifications on virus binding and infection. *Trends Microbiol.* **2016**, *24*, 991−1001.

(9) Li, Z.; Lang, Y.; Liu, L.; Bunyatov, M. I.; Sarmiento, A. I.; de Groot, R. J.; Boons, G. J. Synthetic O-acetylated sialosides facilitate functional receptor identification for human respiratory viruses. *Nat. Chem.* **2021**, *13* (5), 496−503.

(10) Barlow, R. B.; Bremner, J. B.; Soh, K. S. The effects of replacing ester by amide on the biological properties of compounds related to acetylcholine. *Br. J. Pharmacol.* **1978**, *62* (1), 39−50.

(11) Neto, F. R.; Sperelakis, N. Effects of lidocaine, procaine, procainamide and quinidine on electrophysiological properties of cultured embryonic chick hearts. *Br. J. Pharmacol.* **1985**, *86* (4), 817−826.

(12) Bakkers, M. J.; Zeng, Q.; Feitsma, L. J.; Hulswit, R. J.; Li, Z.; Westerbeke, A.; van Kuppeveld, F. J.; Boons, G. J.; Langereis, M. A.; Huizinga, E. G.; de Groot, R. J. Coronavirus receptor switch explained from the stereochemistry of protein-carbohydrate interactions and a single mutation. *Proc. Natl. Acad. Sci. U. S. A.* **2016**, *113* (22), E3111−E3119.

(13) Khedri, Z.; Xiao, A.; Yu, H.; Landig, C. S.; Li, W. Q.; Diaz, S.; Wasik, B. R.; Parrish, C. R.; Wang, L. P.; Varki, A.; Chen, X. A chemical biology solution to problems with studying biologically important but unstable 9-*O*-acetyl sialic acids. *ACS Chem. Biol.* **2017**, *12* (1), 214−224.

(14) Ji, Y.; Sasmal, A.; Li, W.; Oh, L.; Srivastava, S.; Hargett, A. A.; Wasik, B. R.; Yu, H.; Diaz, S.; Choudhury, B.; Parrish, C. R.; Freedberg, D. I.; Wang, L.-P.; Varki, A.; Chen, X. Reversible *O*-acetyl migration within the sialic acid side chain and its influence on protein recognition. *ACS Chem. Biol.* **2021**, *16*, 1951−1960.

(15) Khedri, Z.; Li, Y.; Muthana, S.; Muthana, M. M.; Hsiao, C. W.; Yu, H.; Chen, X. Chemoenzymatic synthesis of sialosides containing C7-modified sialic acids and their application in sialidase substrate specificity studies. *Carbohydr. Res.* **2014**, *389*, 100−111.

(16) Sugiarto, G.; Lau, K.; Qu, J.; Li, Y.; Lim, S.; Mu, S.; Ames, J. B.; Fisher, A. J.; Chen, X. A sialyltransferase mutant with decreased donor hydrolysis and reduced sialidase activities for directly sialylating LewisX. *ACS Chem. Biol.* **2012**, *7* (7), 1232−1240.

(17) Rauvolfova, J.; Venot, A.; Boons, G. J. Chemo-enzymatic synthesis of C-9 acetylated sialosides. *Carbohydr. Res.* **2008**, *343* (10−11), 1605−1611.

(18) Reiding, K. R.; Blank, D.; Kuijper, D. M.; Deelder, A. M.; Wuhrer, M. High-throughput profiling of protein *N*-glycosylation by MALDI-TOF-MS employing linkage-specific sialic acid esterification. *Anal. Chem.* **2014**, *86* (12), 5784−5793.

(19) Muramatsu, W. Chemo- and regioselective monosulfonylation of nonprotected carbohydrates catalyzed by organotin dichloride under mild conditions. *J. Org. Chem.* **2012**, *77* (18), 8083−8091.
(20) McArthur, J. B.; Yu, H.; Zeng, J.; Chen, X. Converting *Pasteurella multocida* α2−3-sialyltransferase 1 (PmST1) to a regioselective α2−6-sialyltransferase by saturation mutagenesis and regioselective screening. *Org. Biomol. Chem.* **2017**, *15* (7), 1700−1709.
(21) Kelm, S.; Madge, P.; Islam, T.; Bennett, R.; Koliwer-Brandl, H.; Waespy, M.; von Itzstein, M.; Haselhorst, T. C-4 modified sialosides enhance binding to siglec-2 (CD22): Towards potent siglec inhibitors for immunoglycotherapy. *Angew. Chem., Int. Ed.* **2013**, *52* (13), 3616−3620.
(22) Weinhold, E. G.; Knowles, J. R. Design and evaluation of a tightly binding fluorescent ligand for influenza A hemagglutinin. *J. Am. Chem. Soc.* **1992**, *114* (24), 9270−9275.
(23) de Groot, R. J. Structure, function and evolution of the hemagglutinin-esterase proteins of corona- and toroviruses. *Glycoconjugate J.* **2006**, *23* (1−2), 59−72.
(24) Zeng, Q.; Langereis, M. A.; van Vliet, A. L.; Huizinga, E. G.; de Groot, R. J. Structure of coronavirus hemagglutinin-esterase offers insight into corona and influenza virus evolution. *Proc. Natl. Acad. Sci. U. S. A.* **2008**, *105* (26), 9065−9069.
(25) Langereis, M. A.; Zeng, Q.; Gerwig, G. J.; Frey, B.; von Itzstein, M.; Kamerling, J. P.; de Groot, R. J.; Huizinga, E. G. Structural basis for ligand and substrate recognition by torovirus hemagglutinin esterases. *Proc. Natl. Acad. Sci. U. S. A.* **2009**, *106* (37), 15897−15902.
(26) Bakkers, M. J.; Lang, Y.; Feitsma, L. J.; Hulswit, R. J.; de Poot, S. A.; van Vliet, A. L.; Margine, I.; de Groot-Mijnes, J. D.; van Kuppeveld, F. J.; Langereis, M. A.; Huizinga, E. G.; de Groot, R. J. Betacoronavirus adaptation to humans involved progressive loss of hemagglutinin-esterase lectin activity. *Cell Host Microbe* **2017**, *21* (3), 356−366.
(27) Deechongkit, S.; Dawson, P. E.; Kelly, J. W. Toward Assessing the Position-Dependent Contributions of Backbone Hydrogen Bonding to β-Sheet Folding Thermodynamics Employing Amide-to-Ester Perturbations. *J. Am. Chem. Soc.* **2004**, *126* (51), 16762−16771.
(28) Gao, J.; Bosco, D. A.; Powers, E. T.; Kelly, J. W. Localized thermodynamic coupling between hydrogen bonding and microenvironment polarity substantially stabilizes proteins. *Nat. Struct. Mol. Biol.* **2009**, *16* (7), 684−690.
(29) Case, D. A.; Betz, R. M.; Cerutti, D. S.; Cheatham, T. E., III; Darden, T. A.; Duke, R. E.; Giese, T. J.; Gohlke, H.; Goetz, A. W.; Homeyer, N.; Izadi, S.; Janowski, P.; Kaus, J.; Kovalenko, A.; Lee, T. S.; LeGrand, S.; Li, P.; Lin, C.; Luchko, T.; Luo, R.; Madej, B.; Mermelstein, D.; Merz, K. M.; Monard, G.; Nguyen, H.; Nguyen, H. T.; Omelyan, I.; Onufriev, A.; Roe, D. R.; Roitberg, A.; Sagui, C.; Simmerling, C. L.; Botello-Smith, W. M.; Swails, J.; Walker, R. C.; Wang, J.; Wolf, R. M.; Wu, X.; Xiao, L.; Kollman, P. A. *AMBER*; University of California: San Francisco, CA, 2016.
(30) Kirschner, K. N.; Yongye, A. B.; Tschampel, S. M.; González-Outeiriño, J.; Daniels, C. R.; Foley, B. L.; Woods, R. J. GLYCAM06: A generalizable biomolecular force field. Carbohydrates. *J. Comput. Chem.* **2008**, *29* (4), 622−655.
(31) Maier, J. A.; Martinez, C.; Kasavajhala, K.; Wickstrom, L.; Hauser, K. E.; Simmerling, C. ff14SB: Improving the accuracy of protein side chain and backbone parameters from ff99SB. *J. Chem. Theory Comput.* **2015**, *11* (8), 3696−3713.
(32) Jorgensen, W. L.; Chandrasekhar, J.; Madura, J. D.; Impey, R. W.; Klein, M. L. Comparison of simple potential functions for simulating liquid water. *J. Chem. Phys.* **1983**, *79* (2), 926−935.
(33) Chandrasekaran, A.; Srinivasan, A.; Raman, R.; Viswanathan, K.; Raguram, S.; Tumpey, T. M.; Sasisekharan, V.; Sasisekharan, R. Glycan topology determines human adaptation of avian H5N1 virus hemagglutinin. *Nat. Biotechnol.* **2008**, *26* (1), 107−113.
(34) Waterhouse, A.; Bertoni, M.; Bienert, S.; Studer, G.; Tauriello, G.; Gumienny, R.; Heer, F. T.; de Beer, T. A P.; Rempfer, C.; Bordoli, L.; Lepore, R.; Schwede, T. SWISS-MODEL: homology modelling of protein structures and complexes. *Nucleic Acids Res.* **2018**, *46* (W1), W296−W303.
(35) Guex, N.; Peitsch, M. C.; Schwede, T. Automated comparative protein structure modeling with SWISS-MODEL and Swiss-PdbViewer: a historical perspective. *Electrophoresis* **2009**, *30*, S162−S173.
(36) Bienert, S.; Waterhouse, A.; de Beer, T. A.; Tauriello, G.; Studer, G.; Bordoli, L.; Schwede, T. The SWISS-MODEL Repository-new features and functionality. *Nucleic Acids Res.* **2017**, *45* (D1), D313−D319.
(37) Lang, Y.; Li, W.; Li, Z.; Koerhuis, D.; van den Burg, A. C. S.; Rozemuller, E.; Bosch, B.-J.; van Kuppeveld, F. J. M.; Boons, G. J.; Huizinga, E. G.; van der Schaar, H. M.; de Groot, R. J. Coronavirus hemagglutinin-esterase and spike proteins coevolve for functional balance and optimal virion avidity. *Proc. Natl. Acad. Sci. U. S. A.* **2020**, *117*, 25759−25770.
(38) Wasik, B. R.; Barnard, K. N.; Ossiboff, R. J.; Khedri, Z.; Feng, K. H.; Yu, H.; Chen, X.; Perez, D. R.; Varki, A.; Parrish, C. R. Distribution of *O*-acetylated sialic acids among target host tissues for influenza virus. *mSphere* **2017**, *2* (5), e00379−16.
(39) Gout, E.; Garlatti, V.; Smith, D. F.; Lacroix, M.; Dumestre-Perard, C.; Lunardi, T.; Martin, L.; Cesbron, J. Y.; Arlaud, G. J.; Gaboriaud, C.; Thielens, N. M. Carbohydrate recognition properties of human ficolins: Glycan array screening reveals the sialic acid binding specificity of M-ficolin. *J. Biol. Chem.* **2010**, *285* (9), 6612−6622.
(40) Kniep, B.; Peter-Katalinić, J.; Flegel, W.; Northoff, H.; Rieber, E. P. CDw 60 antibodies bind to acetylated forms of ganglioside GD3. *Biochem. Biophys. Res. Commun.* **1992**, *187* (3), 1343−1349.
(41) Kiefel, M. J.; von Itzstein, M. Recent advances in the synthesis of sialic acid derivatives and sialylmimetics as biological probes. *Chem. Rev.* **2002**, *102* (2), 471−490.

■ NOTE ADDED AFTER ASAP PUBLICATION

This paper published December 30, 2021 with errors (due to production) in Schemes 1, 2, and 3. The schemes were replaced and the revised paper published with the issue on January 12, 2022.

https://doi.org/10.1021/jacs.1c10329
J. Am. Chem. Soc. 2022, 144, 424−435